

Significance of Image Pre-processing in Computer Vision Based Fire Detection, A Review

Ashwin Rajesh

Abstract—This document describes the most common article elements and how to use the IEEEtran class with LATEX to produce files that are suitable for submission to the IEEE. IEEEtran can produce conference, journal, and technical note (correspondence) papers with a suitable choice of class options.

I. Introduction

WILDFIRES pose a significant threat to humans, wildlife and the environment alike. Left unchecked, A wildfire can spread rapidly causing large scale destruction to forests & infrastructure, as well as releasing large amounts of pollutants into the atmosphere.

Studies have uncovered very strong associations of wildfire smoke with cardiovascular mortality, asthma hospitalisation and further susceptibility to cardiopulmonary effects in elderly adults. The risk of premature death and respiratory morbidity in the general population are also increased due to wildfire smoke [1]. Furthermore, ambient air pollution caused by wildfire smoke has been studied to have adverse affects on children, as a result of their developing lungs and inferior nasal deposition [2]. Breathing in wildfire smoke can cause chest pain and tightness, trouble breathing, dizziness and other symptoms in children [3].

Wildfires have been consuming increasingly large areas of forest globally in recent years, causing vast amounts of damage to the environment in the form of water & air pollution, climate change and destruction of flora and fauna. Sediment exports in water bodies reportedly may increase by up to 1459 times the unburned amount, drastically degrading water quality in the affected areas. [4]. Emissions of airborne particulate matter from wildfires can significant cause significant disruptions to air pollution mitigation targets set by legislation. [5] shows that in high-fire seasons, pollution levels can reach dangerous levels despite aggressive reduction of anthropogenic emissions. An estimated 97000 km² of vegetation was burned in the 2019-2020 Australian bushfires, causing devastating damage to wildlife habitat, with many belonging to species listed at threatened to extinction [6].

Evidently, It has become increasingly crucial to detect wildfires as early as possible to minimize damage to humans and the environment. Current methods of wildfire detection involve three main approaches:

This paper was produced by the IEEE Publication Technology Group. They are in Piscataway, NJ.

Manuscript received April 19, 2021; revised August 16, 2021.

- 1) Terrestrial sensor nodes, which may be placed at fire-prone locations to detect wildfires through environmental readings.
- 2) UAVs can be employed to scan large forest areas and inaccessible terrain.
- 3) Satellite based systems can cover vast areas of land and determine the extent and direction of wildfires.

Despite the various classifications of technologies within wildfire detection, advancements in computer vision object detection has spurred use in terrestrial, aerial as well as satellite systems. [7] explores the feasibility of space-borne fire detection using onboard computer vision to rapidly generate alerts. The traditional method of downloading image data from satellites has too much latency for time-sensitive applications such as fire detection. By examining performance of hardware accelerators for edge computing such as Nvidia Jetson and Movidius Myriad 2, the report found that AI inference on-board the satellite is possible in terms of performance as well as power consumption, allowing for low latency detection of wildfires. [8] details methods to optimise Deep Learning to deal with UAV limitations such as image degradation, small fire size & background complexity. By combining EfficientNet-B5, vision transformers and EfficientSeg convolutional model, an accuracy of 85.12% was obtained, outperforming many state-of-the-art models. [9] proposes a low cost WSN fire detection approach based on YOLO object detection models. The system, named SDFS was trained on a dataset of 26,520 images and achieved a high precision rate of 97.1% for smoke and fire classification.

Due to the importance of computer vision based object detection in wildfire detection, it is imperative that they are as accurate as possible. There are many different techniques to improve the performance of neural networks. Transfer learning is the process of using a model that has been pre-trained on a large dataset and further training and fine tuning it to a specific task. [10] studies the impact of transfer learning on classification by comparing six different pre-trained architectures. The models were trained using an open access dataset of 3886 images and found that all six architectures were able to achieve a testing accuracy of above 90% despite a relatively small training dataset. Augmenting data with synthetically generated samples investigated by [11] found that inserting data-space transformations such as warped images provided improved performance and reduced overfitting. [12] proposed an image pre-processing pipeline using advanced

techniques such as HSV filters and corner detection to assist models with classification by eliminating unwanted noise in images. This method has observed to improve fire detection accuracy by 5.5% and smoke detection by 6% in object detection models.

However, detecting smoke and fire can prove challenging to a neural network model for a variety of reasons. Uneven and dim lighting conditions can pose substantial difficulties while detecting smoke edges in an image. The inconsistent shape and colour of fire as well as smoke can further cause complications. Xin et al. [13] employs the use of a deep ResNet architecture in order to tackle this issue. Accurately and consistently detecting smoke, as a result, tends to require deeper models that are capable of learning complex features. Wildfire detection is often performed in remote terrestrial regions, aerially or from space, which will limit the computational power available for running neural networks. Additionally, the network must maintain real-time inference, as latency is critical in detecting fires as early as possible. These factors make larger complex neural networks suboptimal for wildfire detection. Therefore, a solution to real-time smoke detection that can be powered by low-specification edge computing devices such as a Raspberry Pi must be explored.

This report aims to explore different methods employed in improving the performance and efficiency of wildfire detection systems, with a focus on computer vision based fire detection using Convolutional Neural Networks (CNNs). Fire and smoke detection is carried out through a variety of mediums, such as terrestrial sensor nodes, UAV scanning and satellite based approaches. Observing the literature, it is apparent that computer vision plays a significant role in all systems, making it important to maximise their efficiency and accuracy. Furthermore, it is important to optimise such systems to run on low-powered edge computing devices, which are currently used to detect wildfires. To this end, a multitude of image preprocessing filters relevant to smoke detection were explored. A pipeline of processing that involves Dark Channel Prior in combination with smoke edge detection with Sobel kernels is proposed and benchmarked in this report. The proposed dark channel prior + edge detection algorithm aims to improve on existing methods of smoke preprocessing using DCP detailed in [12]. Specifically, false positives due to high light intensity artifacts in the image such as the sky are significantly mitigated, thanks to edge detection filters revealing characteristics that are unique to smoke.

The benchmarks are carried out on a Raspberry Pi 4B, to simulate low-powered edge computing hardware that is consistently used in terrestrial, UAV and satellite systems. Large deep-learning networks are unviable on these systems due to the high computational intensity, while models with reduced parameters are more efficient but suffer from less accurate inference. The preprocessing pipeline aims to improve the accuracy of lightweight models by highlighting important features in fire and

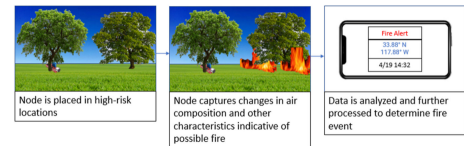


Fig. 1: Basic operation of WSNs. Images sourced from Creative Commons, following the guidelines on Attribution 3.0 Unported, CC By 3.0

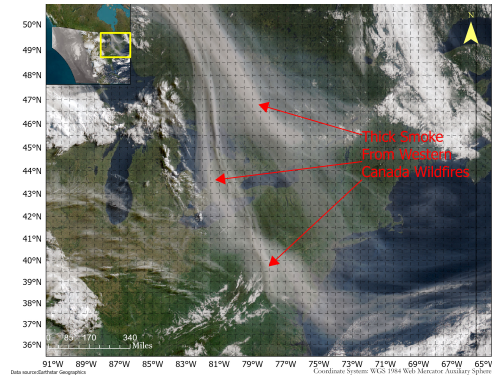


Fig. 2: Satellite Based Wildfire Detection

smoke, while reducing unwanted noise in the image. To this end, a YOLOv8 nano model is trained on an open source Wildfire Smoke Detection dataset [14]. This model is compared with another model that has been trained on the exact same dataset, but with the smoke enhancing preprocessing pipeline stated above.

II. Literature Review

Edge computing sensor nodes can be placed at high risk locations that can monitor temperature, humidity and other characteristics of air in the surrounding area. These systems generally use a microcontroller to operate sensors, relying on solar cells for long-term power. By setting up multiple such nodes in different areas forming a Wireless Sensor Network (WSN), the collected sensor data may then be analyzed to determine the locations of fire events [15]. More advanced methods of data classification with the use of artificial neural networks boast a high accuracy of >82% with multiple sensors [16]. The low cost of WSN systems has made it an increasingly popular choice for real-time monitoring of forest fires. However, sensor nodes fail to be viable in some situations. Establishing wireless communications for a WSN can prove challenging in rural or untamed areas such as forests [9]. The sensor nodes may also be prone to damage from the wildfire, needing to be replaced in order to continue using the system.

UAVs have seen extensive research for this application, as they provide valuable visual data which can be employed to carry out search and rescue operations, save forest resources, help firefighters navigate efficiently among numerous other enhancements. Rather than sending ground crews to monitor hazardous environments, UAVs can drastically reduce the risk to firefighting crews



Fig. 3: Example of Image filtered using the described HSV mask. (a) Original image. (b) Filtered image.

by remotely scanning large amounts of dangerous forest area. However UAVs tend to perform poorly in harsh weather conditions, have limited flight time and require a human operator to have a visual line of sight [17]. These factors combined with expensive operation costs severely limit the effectiveness of UAVs in many circumstances.

Satellite-based fire detection can potentially offer significant advantages over traditional methods due to the vast areas they can monitor. The benefits and limitations of these systems largely depend on the satellite's orbit. Satellites in Sun-Synchronous Orbit (SSO) provide high spatial resolution but revisit the same location only after several days, resulting in low temporal resolution. This delay makes SSO satellites less effective for real-time wildfire detection [7]. In contrast, Geostationary Earth Orbit (GEO) satellites remain fixed over the same region, as their orbital period matches Earth's rotation. Equipped with multispectral imaging sensors, GEO satellites provide continuous monitoring, making them ideal for detecting and tracking fires in real time.

A. Image Pre-Processing Algorithms

1) HSV filter: Hue, Saturation, Value (HSV) is a cylindrical-coordinate representation of points in an RGB colour model. It is an alternative representation of the RGB color model that intends to describe colors in a way that is more aligned with human perception. Colour masks can be created by setting upper and lower bounds within the HSV channels. This can then be applied to an image to filter specific tones of colour. A study by [18] utilized HSV thresholding to detect human skin in an image. The process achieved an impressive 99.587% accuracy on natural images under varying light conditions. [12] used a HSV filter in addition to other preprocessing stages to isolate colours of fire in an image to assist object detection models with inference, which resulted in a 5.5% increase in fire detection accuracy. The following bounds were used to preprocess images in the paper:

$$\text{RoI}_{\text{HSV}(x,y)} := \begin{cases} 1, & 20 < H(x,y) < 40 \\ & \text{and } 50 < S(x,y) < 255 \\ & \text{and } 50 < V(x,y) < 255 \\ 0, & \text{otherwise} \end{cases}$$

2) Edge & Contour Detection: Edge detection involves identifying regions of an image where the contrast between pixels changes dramatically. Capturing edges can be used to reveal important properties in the image as these edges often correspond to changes in depth, illumination, orientation or material. Edge detection can be particularly useful in detecting fire, as it uncovers data about positions of contours and contrasts where fire and smoke could potentially exist. More specifically, method to use low edge responses in an image region may be useful in differentiating between smoke and sky. This method is explored further in this paper

Edge detection has seen use in many fields to extract valuable information from visual data. [19] aims to accurately detect COVID-19 patients by using edge detection to improve detection accuracy of a CNN on CT images of the lungs. The addition of sobel edge detection to a CNN proved to be an effective approach, achieving an accuracy of 99.02% on a custom dataset. [20] proposes an approach to detect roads in satellite images using edge detection and semantic-segmentation. The results showed accurate segmentation & edge detection even in complicated backgrounds. This shows the potential of edge detection in satellite and UAV based systems, where small details in an image are of significant importance.

A popular method of edge detection thanks to its computational simplicity is the Sobel operator. The sobel filter involves convolving the image with a specific kernel which calculates the gradient of the image in x and y directions [21]. For a given image, let us consider a pixel region such as in figure 4.

The figure shows the value in each cell is the brightness of the pixel in that position within the image. In the region shown above, we can see that the pixel brightness rapidly changes between the 2nd and 3rd columns, which would be perceived as an edge by humans. We can then convolve the gradient filter shown in figure 5 over each pixel of the image.

Let us consider the pixel in the second column and second row as the pixel currently being processed. Each value in the gradient filter is multiplied with the corresponding pixel in the neighbouring 3x3 area around our center pixel, and summed. In our example, this would output a high value of 200, as our area of interest contains high intensity

50	50	100	100
50	50	100	100
50	50	100	100
50	50	100	100

Fig. 4: Pixel region where numbers indicate brightness of the pixel

1	0	1
-2	0	-2
1	0	1

Fig. 5: Pixel region where numbers indicate brightness of the pixel

pixels on the right and lower intensity on the left.

This process is repeated with every other pixel to produce the partial derivative of the image in the x direction. By obtaining the y partial derivative in a similar manner, we may combine the images to produce a resultant image containing high absolute values near edges and a value close to 0 everywhere else. The x and y gradients can be combined using the following method:

$$G = \sqrt{G_x^2 + G_y^2}$$

Where G is the positive magnitude of the intensity of an edge at that pixel. Pixels with small edge response will have a value closer to 0 (black) while pixels around an edge will have a high value and appear white. The effects of a sobel filter on an image can be seen in figure 6, where most of the scenery and smoke is covered in many white lines, while the small area of sky above is almost completely dark.

3) Corner Detection: Corner detection is a common technique used in computer vision to infer features from an image. [12] shows that a corner detection algorithm is a vital preprocessing stage, as it separates fire from other objects of similar color, which would fall within the thresholds of a HSV filter. The popular Harris corner detector uses the autocorrelation function of the image to determine intensity differences within patches of an image. Using a Taylor expansion, the autocorrelation function can be approximated as [12] [22]:

$$I(x_i, y_i) + [I_{x(x_i, y_i)} I_{y(x_i, y_i)}] \begin{pmatrix} u \\ v \end{pmatrix}$$

Where I represents intensity and u and v represent the shift in the region from the reference pixel (x_i, y_i) . This shows that the change in intensity depends on the partial derivatives I_x and I_y of the image. When written in matrix form, the expression is as follows:



(a)



(b)

Fig. 6: Image with smoke processed using a basic sobel filter

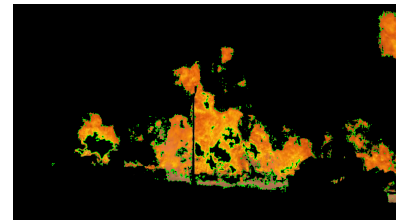


Fig. 7: Corner detection executed on HSV-filtered image of fire (corners marked green)

$$M = \begin{pmatrix} \sum(I_{x(x_i, y_i)}^2) & \sum(I_{x(x_i, y_i)} I_{y(x_i, y_i)}) \\ \sum(I_{x(x_i, y_i)} I_{y(x_i, y_i)}) & \sum(I_{y(x_i, y_i)}^2) \end{pmatrix}$$

The eigenvalues of the matrix can be found using the determinant and trace:

$$\det(M) = AB - C^2 = \lambda_1 \lambda_2$$

$$\text{trace}(M) = A + B = \lambda_1 + \lambda_2$$

There are three possible situations based on their values:

- Both eigenvalues are small: this happens when the pixels are in a flat region
- One eigenvalue is bigger than the other eigenvalue: The region likely is an edge
- Both eigenvalues are large: the region is a corner

Therefore, corner regions within an image will output a high corner strength. These regions can be used as a candidate region that can be inferred through a CNN.

4) Dark Channel Prior: Dark Channel Prior has been commonly used to measure the degree of haziness as well as haze-removal in images. The technique is based on the observation that in most outdoor images, pixels tend to have low intensities in atleast one colour channel (dark channel). This property can be used to estimate the transmission map of an image, representing the amount of haze affecting the scene. Atmospheric haze can be modelled as follows [23]:

$$I(x) = J(x)t(x) + A(1 - t(x))$$

$I(x)$ represents a pixel that reached the camera. $J(x)$ represents the undistorted pixel. $t(x)$ is the transmission map, representing how much scene radiance is retained, where a value of 1 means no haze and 0 means maximum haze. Due to the scattering of light from haze, low intensity channels in hazy patches of an image have an inherently higher value. As a result, DCP can be used to estimate $t(x)$ providing the areas of the image affected by haze. [12] and [24] note that dark channel prior methods can apply to smoke due to the similar nature, having relatively higher values in their dark channels. This causes smoke to be picked up as an area of high haze in the transmission map. [12] apply a threshold to the transmission map, extracting areas with high dark channel values and suppressing the rest. As a result, a 6% increase in detection accuracy was achieved compared to detection without extra preprocessing stages.

As shown in figure 8, DCP reveals areas with high intensity values in all three channels, causing haze, smoke, and sky regions to appear very bright compared to the rest in the second image. In the third image, regions below a certain intensity threshold are suppressed to zero. This gives us the regions where there is a high chance of smoke or fog.

Despite the notable improvements in smoke detection using dark channel prior, there are some drawbacks to be considered. Dark channel prior tends to be unreliable when the image consists of a large portion of sky, since the sky tends to have a high dark channel value, causing the algorithm to mistake it as hazy or smoky area. This is evident in figure 8, where the sky is included in the final thresholded output image.

5) Histogram Equalization: Histogram Equalization increases the global contrast in images, which can enhance the visibility of finer details within an image. The algorithm spreads the intensity values out in an image so that it utilizes the full range of values more efficiently [25]. As a result, HE is most effective on images with a narrow range of intensity values.

HE's effectiveness at enhancing image quality makes it a practical technique in many scenarios. [26] presents a system to detect early fires inside a ship using a YOLO computer vision model. Images were preprocessed with Histogram Equalization to reduce the impact of water vapour on the quality of the images, contributing to the remarkable 99% accuracy of the model. [27] investigates



(a)



(b)

Fig. 8: Image processed with Dark channel prior & thresholded to high intensity values (a) Original image (b) Dark channel processed image

using CLAHE, an advanced form of histogram equalization along with a YOLOv4 model to detect bone fracture features in xray images, obtaining a result of 81.91% when trained on a small dataset.

Let us consider n_i as the number of occurrences of the gray level i in a greyscale image. The probability of a pixel with level i is as follows:

$$p(i) = \frac{n_i}{n}, 0 \leq i < L$$

Where L is the total number of gray levels in the image. The cumulative distribution function can then be defined:

$$cdf(i) = \sum_{j=0}^L p(j)$$

In order to achieve a flat histogram of values, the CDF must be linearized. This can be carried out by the following equation:

$$h(v) = \text{round} \left(\frac{cdf(v) - cdf_{\min}}{N - cdf_{\min}} \right)$$

Where N is the number of pixels in the image.

By applying this function to each pixel of the original image, we obtain a resulting image with a flatter histogram of intensities, increasing contrast and visibility in the image. An example of this contrast enhancement is shown in figure 9.

III. An Improved Smoke Detection System

Using Dark Channel Prior to preprocess images has proven to be worthwhile for improving detection accuracy [24] [28]. By isolating smoke areas from other background



(a)



(b)

Fig. 9: Histogram equalization on image

noise in the image, DCP simplifies classification for a neural network, allowing for better results on smaller datasets and shallower, faster models. However, DCP fails to be effective in images that contain other artifacts of high light-intensity, such as the sky. This could cause inconsistent results particularly in terrestrially placed detection nodes, where the camera might have small parts of the sky in frame.

Generally, we can assume that smoke in an image is more noisy and contains contours and textures that a plain sky would not have. This texture can be picked up by a Sobel operator in an edge response image. The response image may be used to identify areas with very little edge response which can safely be eliminated from consideration.

In order to eliminate certain areas of an image from being considered in the DCP algorithm, a binary threshold can be used on the image, which will either suppress pixels to zero or change them to max value depending on a thresholding condition. This can be useful for creating a map of unwanted sections in an image that can be suppressed at a later stage. We can provide the Sobel filtered image to a binary threshold to suppress only parts of the image which have an edge response very close to 0. The resulting image mask would be black in sky areas, allowing us to effectively detect sky regions.

In figures 10 and 11, A sobel filter as well as dark channel prior image is computed from the original image. The edge response image is generously dilated and blurred in order to mitigate small dark spots in the image as they are irrelevant. After applying a binary threshold, this image is used on the DCP output to suppress the pixel regions of sky.

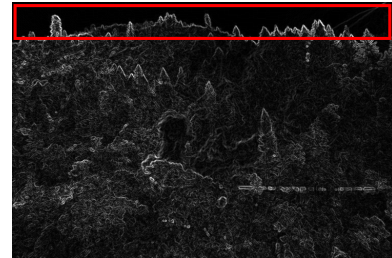


Fig. 10: The sobel edge filter has close to zero response on sky regions

IV. Drawbacks

The proposed Sobel/DCP method eliminates sky regions from an image in most cases. However the performance may be inconsistent in certain conditions such as cloudy skies or the presence of black smoke. In certain situations where the sky is partially cloudy, clouds may take up a similar shape and texture to early wildfire smoke, scattering light in a similar way causing the algorithm to classify it as a positive region for the existence of smoke. Black smoke, usually associated with the combustion of fuels is missed by the algorithm as it's dark channel light intensity falls lower than the algorithm's threshold.

The Sobel/DCP algorithm's downsides indicates effectiveness specifically at white or light gray smoke. Darker smokes have the propensity to have light intensities that are too low for the algorithm to notice. Studies have linked light gray and white smoke with smouldering fires or those in early stages [29]. The proposed algorithm could prove to be useful at early wildfire detection, allowing a wildfire response team to be notified faster, potentially preventing a larger disaster.

V. Experimental Results

The dark channel edge detection system was tested on various images as well as on a large smoke & fire dataset to benchmark speed & computational intensity, which are important in edge computing systems. The tested images show that the algorithm effectively separated smoke from sky and other unwanted noise, also being able to suppress the image completely in cases of no detected smoke or haze.

Notable weak points of the algorithm include differentiation between smoke and clouds. Smaller clouds with visible edges and contours can appear similar, which may reduce the algorithm's accuracy. Darker smoke such as those from burning fossil fuels are not easily detected by the edge + dcp algorithm. Since dark channel prior favours high light intensity values, dark gray or black smoke does not have any characteristics that DCP can detect.

References

- [1] Y. Lei, T.-H. Lei, C. Lu, X. Zhang, and F. Wang, "Wildfire smoke: Health effects, mechanisms, and mitigation," *Environmental Science & Technology*, vol. 58, no. 48, pp. 21 097–21 119, 2024, pMID: 39516728. [Online]. Available: <https://doi.org/10.1021/acs.est.4c06653>

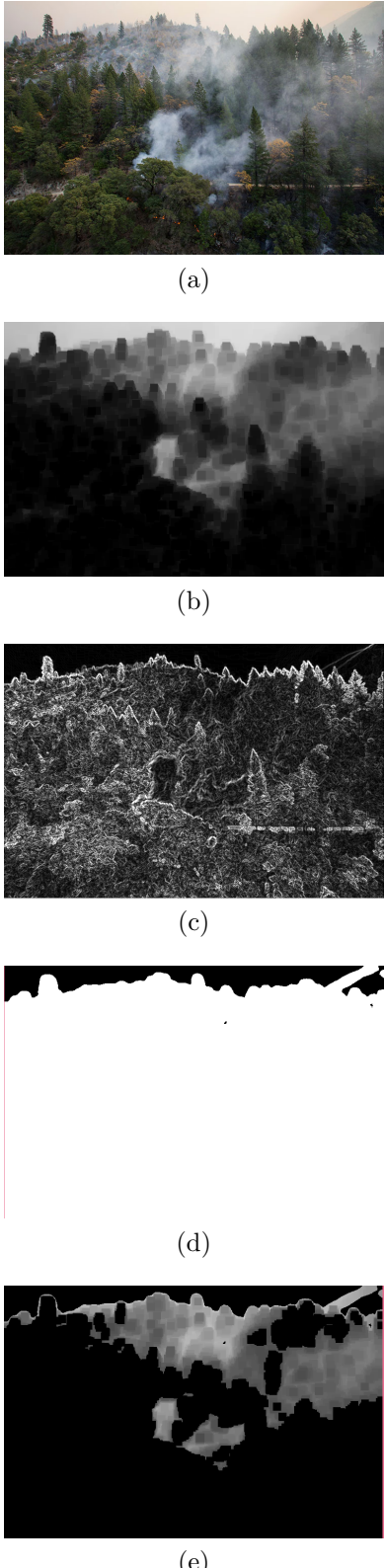


Fig. 11: Edge Detection & DCP Filtering to detect smoke without conflating sky regions (a) Original image. (b) DCP processed image. (c) Sobel filtered image. (d) Sky filter by dilating the sobel output. (e) Thresholded DCP image combined with sky filter, leaving only smoke regions.

- [2] S. M. Holm, M. D. Miller, and J. R. Balmes, "Health effects of wildfire smoke in children and public health tools: a narrative review," *Journal of Exposure Science and Environmental Epidemiology*, vol. 31, no. 1, pp. 1–20, 02 2021, copyright - © The Author(s) 2020; Last updated - 2024-10-07; SubjectsTermNotLitGenreText - Social. [Online]. Available: <http://ezproxy.lib.uts.edu.au/login?url=https://www.proquest.com/scholarly-journals/health-effects-wildfire-smoke-children-public/docview/2476043836/se-2>
- [3] "Protecting children from wildfire smoke and ash."
- [4] H. G. Smith, G. J. Sheridan, P. N. Lane, P. Nyman, and S. Haydon, "Wildfire effects on water quality in forest catchments: A review with implications for water supply," *Journal of Hydrology*, vol. 396, no. 1, pp. 170–192, 2011. [Online]. Available: <https://www.sciencedirect.com/science/article/pii/S0022169410006748>
- [5] W. Knorr, F. Dentener, J.-F. Lamarque, L. Jiang, and A. Arnette, "Wildfire air pollution hazard during the 21st century," *Atmospheric chemistry and physics*, vol. 17, no. 14, pp. 9223–9236, 2017.
- [6] M. Ward, A. I. T. Tulloch, J. Q. Radford, B. A. Williams, A. E. Reside, S. L. Macdonald, H. J. Mayfield, M. Maron, H. P. Possingham, S. J. Vine, J. L. O'Connor, E. J. Massingham, A. C. Greenville, J. C. Z. Woinarski, S. T. Garnett, M. Lintermans, B. C. Scheele, J. Carwardine, D. G. Nimmo, D. B. Lindenmayer, R. M. Kooyman, J. S. Simmonds, L. J. Sonter, and J. E. M. Watson, "Impact of 2019–2020 mega-fires on australian fauna habitat," *Nature ecology & evolution*, vol. 4, no. 10, pp. 1321–1326, 2020.
- [7] K. Thangavel, D. Spiller, R. Sabatini, S. Amici, S. T. Sasidharan, H. Fayek, and P. Marzocca, "Autonomous satellite wildfire detection using hyperspectral imagery and neural networks: A case study on australian wildfire," *Remote Sensing*, vol. 15, no. 3, 2023. [Online]. Available: <https://www.mdpi.com/2072-4292/15/3/720>
- [8] R. Ghali, M. A. Akhloufi, and W. S. Mseddi, "Deep learning and transformer approaches for uav-based wildfire detection and segmentation," *Sensors (Basel, Switzerland)*, vol. 22, no. 5, pp. 1977–, 2022.
- [9] F. M. Talaat and H. ZainEldin, "An improved fire detection approach based on yolo-v8 for smart cities," *Neural Computing and Applications*, vol. 35, no. 28, pp. 20939–20954, Oct 2023. [Online]. Available: <https://doi.org/10.1007/s00521-023-08809-1>
- [10] S. Asif, Y. Wenhui, K. Amjad, H. Jin, Y. Tao, and S. Jinhai, "Detection of covid-19 from chest x-ray images: Boosting the performance with convolutional neural network and transfer learning," *Expert systems*, vol. 40, no. 1, 2023.
- [11] S. C. Wong, A. Gatt, V. Stamatescu, and M. D. McDonnell, "Understanding data augmentation for classification: When to warp?" in *2016 International Conference on Digital Image Computing: Techniques and Applications (DICTA)*. IEEE, 2016, pp. 1–6.
- [12] J. Ryu and D. Kwak, "A study on a complex flame and smoke detection method using computer vision detection and convolutional neural network," *Fire*, vol. 5, no. 4, 2022. [Online]. Available: <https://www.mdpi.com/2571-6255/5/4/108>
- [13] X. Wang, J. Wang, L. Chen, and Y. Zhang, "Improving computer vision-based wildfire smoke detection by combining se-resnet with svm," *Processes*, vol. 12, no. 4, pp. 747–, 2024.
- [14] G. Jocher, A. Chaurasia, and J. Qiu, "Ultralytics yolov8," 2023. [Online]. Available: <https://github.com/ultralytics/ultralytics>
- [15] A. Mohapatra and T. Trinh, "Early wildfire detection technologies in practice—a review," *Sustainability*, vol. 14, no. 19, pp. 12270–, 2022.
- [16] X. Yan, H. Cheng, Y. Zhao, W. Yu, H. Huang, and X. Zheng, "Real-time identification of smoldering and flaming combustion phases in forest using a wireless sensor network-based multi-sensor system and artificial neural network," *Sensors*, vol. 16, no. 8, 2016. [Online]. Available: <https://www.mdpi.com/1424-8220/16/8/1228>
- [17] F. Afghah, "Autonomous unmanned aerial vehicle systems in wildfire detection and management-challenges and opportunities," in *Dynamic Data Driven Applications Systems*, E. Blasch, F. Damera, and A. Aved, Eds. Cham: Springer Nature Switzerland, 2024, pp. 386–394.

- [18] E. K. Hassan and J. H. Saud, "Hsv color model and logical filter for human skin detection," in AIP Conference Proceedings, vol. 2457, no. 1. Melville: American Institute of Physics, 2023.
- [19] D. Sharifrazi, R. Alizadehsani, M. Roshanzamir, J. H. Joloudari, A. Shoeibi, M. Jafari, S. Hussain, Z. A. Sani, F. Hasanzadeh, F. Khozeimeh, A. Khosravi, S. Nahavandi, M. Panahiazar, A. Zare, S. M. S. Islam, and U. R. Acharya, "Fusion of convolution neural network, support vector machine and sobel filter for accurate detection of covid-19 patients using x-ray images," *Biomedical Signal Processing and Control*, vol. 68, p. 102622, 2021. [Online]. Available: <https://www.sciencedirect.com/science/article/pii/S1746809421002196>
- [20] H. Ghandoorh, W. Boulila, S. Masood, A. Koubaa, F. Ahmed, and J. Ahmad, "Semantic segmentation and edge detection—approach to road detection in very high resolution satellite images," *Remote sensing (Basel, Switzerland)*, vol. 14, no. 3, pp. 613–, 2022.
- [21] I. Sobel, "An isotropic 3x3 image gradient operator," Presentation at Stanford A.I. Project 1968, 02 2014.
- [22] J. Sánchez, N. Monzón, and A. Salgado, "An Analysis and Implementation of the Harris Corner Detector," *Image Processing On Line*, vol. 8, pp. 305–328, 2018, <https://doi.org/10.5201/ipol.2018.229>.
- [23] K. He, J. Sun, and X. Tang, "Single image haze removal using dark channel prior," *IEEE transactions on pattern analysis and machine intelligence*, vol. 33, no. 12, pp. 2341–2353, 2011.
- [24] Y. Liu, W. Qin, K. Liu, F. Zhang, and Z. Xiao, "A dual convolution network using dark channel prior for image smoke classification," *IEEE Access*, vol. 7, pp. 60 697–60 706, 2019.
- [25] S. Patel and M. Goswami, "Comparative analysis of histogram equalization techniques," in 2014 International Conference on Contemporary Computing and Informatics (IC3I), 2014, pp. 167–168.
- [26] A. Ergasheva, F. Akhmedov, A. Abdusalomov, and W. Kim, "Advancing maritime safety: Early detection of ship fires through computer vision, deep learning approaches, and histogram equalization techniques," *Fire*, vol. 7, no. 3, p. 84, 2024, copyright - © 2024 by the authors. Licensee MDPI, Basel, Switzerland. This article is an open access article distributed under the terms and conditions of the Creative Commons Attribution (CC BY) license (<https://creativecommons.org/licenses/by/4.0/>). Notwithstanding the ProQuest Terms and Conditions, you may use this content in accordance with the terms of the License; Last updated - 2024-10-03; SubjectsTermNotLitGenreText - Social. [Online]. Available: <http://ezproxy.lib.uts.edu.au/login?url=https://www.proquest.com/scholarly-journals/advancing-maritime-safety-early-detection-ship/docview/3001523245/se-2>
- [27] H. P. Nguyen, T. P. Hoang, and H. H. Nguyen, "A deep learning based fracture detection in arm bone x-ray images," in 2021 International Conference on Multimedia Analysis and Pattern Recognition (MAPR), 2021, pp. 1–6.
- [28] D.-K. Kwak and J.-K. Ryu, "A study on the dynamic image-based dark channel prior and smoke detection using deep learning," *Journal of electrical engineering & technology*, vol. 17, no. 1, pp. 581–589, 2022.
- [29] H.-Y. Jang and H. Cheol-Hong, "Preliminary study for smoke color classification of combustibles using the distribution of light scattering by smoke particles," *Applied Sciences*, vol. 13, no. 1, p. 669, 2023, copyright - © 2023 by the authors. Licensee MDPI, Basel, Switzerland. This article is an open access article distributed under the terms and conditions of the Creative Commons Attribution (CC BY) license (<https://creativecommons.org/licenses/by/4.0/>). Notwithstanding the ProQuest Terms and Conditions, you may use this content in accordance with the terms of the License; Last updated - 2024-05-07; SubjectsTermNotLitGenreText - South Korea. [Online]. Available: <http://ezproxy.lib.uts.edu.au/login?url=https://www.proquest.com/scholarly-journals/preliminary-study-smoke-color-classification/docview/2761155047/se-2>